# PR inhibition stimulates G6PD expression to enhance malignancy in luminal breast cancer

Janghee Lee

The Graduate School
Yonsei University
Department of Medicine

# PR inhibition stimulates G6PD expression to enhance malignancy in luminal breast cancer

A Dissertation Submitted
to the Department of Medicine
and the Graduate School of Yonsei University
in partial fulfillment of the
requirements for the degree of
Doctor of Philosophy in Medical Science

Janghee Lee

December 2024

**This certifies that the Dissertation of Janghee Lee is approved**

Thesis Supervisor Sung Gwe Ahn

Thesis Committee Member Sungsoon Fang

Thesis Committee Member Sae Byul Lee

Thesis Committee Member Yoon Jin Cha

Thesis Committee Member Jinhyuk Bhin

**The Graduate School**
**Yonsei University**
**December 2024**

## ACKNOWLEDGEMENTS

I would like to express my deepest gratitude to all those who have supported me throughout the completion of this thesis. First and foremost, I extend my sincerest thanks to my advisor, Professor Sung Gwe Ahn, for invaluable guidance, encouragement, and expertise throughout the course of my research. Their insights have been instrumental in shaping this work. I am also deeply grateful to the members of my thesis committee, Professors Sungsoon Fang, Sae Byul Lee, Yoon-Jin Cha and Jinhyuk Bhin, for their thoughtful feedback and constructive criticism, which greatly contributed to the improvement of this thesis. I would like to acknowledge my colleagues and co-authors, Jae Woong Jeong in the Yonsei university college of medicine/Department of medicine and Hae-Kyung Lee in the Severance biomedical science institute, Gangnam severance hospital for their constant support and fruitful discussions, which enriched both my research and my experience. A special thanks goes to Institute for breast cancer precision medicine, Gangnam severance hospital for their technical assistance and dedication. Lastly, I am deeply thankful to my family and friends for their unwavering support, patience, and encouragement, without which this journey would not have been possible. To all who contributed to the completion of this work, I offer my heartfelt thanks.

# TABLE OF CONTENTS

# LIST OF FIGURES

# ABSTRACT

## PR inhibition stimulates G6PD expression to enhance malignancy in luminal breast cancer

Luminal breast cancer is the most prevalent and prognostic subtype of breast cancer. However, it has been reported that luminal breast cancer patients with lower progesterone receptor (PR) expression are associated with poor survival outcomes. Nevertheless, there is insufficient evidence linking PR expression to an aggressiveness of luminal breast cancer. We were motivated by previous studies showing that PR and standardized uptake value (SUV) on [$^{18}$F] fluorodeoxyglucose positron emission tomography (FDG-PET) have an inverse correlation, and aimed to identify a potential link between PR expression and glucose metabolism, particularly the pentose phosphate pathway (PPP). To investigate it, we performed a single cell RNA sequencing (scRNA-seq) analysis using published dataset. Interestingly, the analysis revealed that specific epithelial cells with both increased proliferation activity and decreased PR expression, which increased activity of the PPP and glucose-6-phosphate dehydrogenase (G6PD) expression. To verify these findings, we silenced PR expression in luminal breast cancer cell lines, MCF7 and T47D, which resulted in accelerated proliferation and PPP activity with G6PD expression. We hypothesized that PR knockdown (KD) increases breast cancer aggressiveness by boosting glucose utilization with PPP activity. Importantly, treatment with G6PD inhibitor (G6PDi), a G6PDi reduced aggressiveness of PR KD cancer cells. These findings suggest that targeting G6PD could be a promising therapeutic strategy to suppress the aggressiveness of luminal breast cancer, using low PR expression as a biomarker.

---

Key words : luminal breast cancer, progesterone receptor, glucose-6-phosphate dehydrogenase

# 1. INTRODUCTION

Breast cancer, one of the most prevalent cancers worldwide, is clinically categorized into four subtypes. It is divided into luminal A, luminal B, human epidermal growth factor receptor 2 (HER2)-positive and triple negative breast cancer, determined by immunohistochemical intensity hormone receptors and HER2 [1]. Luminal breast cancer including luminal A and B, characterized by estrogen receptor (ER)-positive and HER2-negative, is the most common breast cancer subtype and is known to have better prognosis compared to other subtypes [2-4]. However, concern such as late recurrence still exist for these patients, highlighting the ongoing need for novel therapeutic strategies [5].

It has been well known that the progesterone receptor (PR) is associated with prognosis in ER-positive/HER2-negative breast cancer. Previous clinical studies have reported that tumors without PR expression increase recurrence and mortality rates compared to tumors with PR expression [6, 7]. Furthermore, the PR gene is included in the 21-multigene assay [8, 9], a standard test for predicting the benefit of chemotherapy in ER-positive/HER2-negative breast cancer, and it has been demonstrated that there is inverse correlation between PR expression and the recurrence score (RS) of 21-multigene assay (Oncotype DX®) [10]. However, the mechanism of PR as a prognostic factor has not been clearly elucidated.

Our previous findings revealed an inverse correlation between PR expression and standardized uptake value (SUV) on [$^{18}$F] fluorodeoxyglucose positron emission tomography (FDG-PET) scans [10, 11]. This suggests a potential link between low PR levels, increased glucose uptake, and aggressiveness of breast cancer [12]. Elevated glucose uptake, as indicated by high SUV, implicates reliance of cancer cells on glycolysis for energy production [13].

The pentose phosphate pathway (PPP), the parallel pathway to glycolysis, is crucial for managing oxidative stress through NADPH generation [14]. The PPP is activated in human cancer tissues, and is known to enhance the malignant potential of cancer cells, including cell proliferation, tumor invasion, and therapy resistance [15]. Importantly, high glucose-6-phosphate dehydrogenase (G6PD), the key enzyme of PPP, expression correlates with poor prognosis in breast cancer patients [16, 17]. Given the association between low PR, increased glucose utilization, and aggressiveness of breast cancer, we hypothesized that low PR expression in luminal breast cancer might activate the PPP through G6PD.

In this study, we investigated the relation between PR and breast cancer malignancy and determined which signaling pathways influence the aggressiveness in cancer cells. Interestingly, we

found aggressive luminal epithelial cells with low PR enriched with PPP. To verify it in vitro, we silenced PR on luminal breast cancer cell lines and performed bulk mRNA sequencing (bulk RNA-seq), finding up-regulation of G6PD expression. Decisively, treatment of a selective inhibitor of G6PD (G6PDi) [18], on PR knockdown (KD) cells induced a decreased cell growth rate. These findings suggest that G6PD might be a novel target in luminal patients with low PR expression as a biomarker.

# 2. MATERIALS AND METHOD

## 2.1. scRNA-seq analysis

The matrices of luminal breast cancer patients from GSE161529 [19] and GSE176078 [20] were collected and input using Seurat package (v.4.3.0) in R. Seurat objects were constructed and they were processed through filtering out low-quality cells, excluding less than 1,000 cells and normalizing the data. The remaining Seurat objects were integrated into one object containing around 100,000 cells using 'IntegrateData' function. The integrated Seurat object was performed 'RunPCA' function to reduce the dimensions to visualized on two-dimension using 'RunUMAP' function. The identified eight clusters were divided by 'FindNeighbors' and 'FindClusters' function. The Integrated Seurat object was visualized using 'DimPlot', 'DotPlot', 'VlnPlot', 'FeaturePlot'. Amont eight clusters, epithelial cell cluster was subset using 'subset'. The cell cycle score analysis was conducted using 'CellCycleScoring'. The escape package (v.1.4.0) [21] in R was used to estimate the normalized enrichment score (NES) and false discovery rate (FDR) of the PPP gene set. The subsetted epithelial cell cluster was conducted by copy number variation (CNV) analysis using CopyKAT package (v. 1.1.0) in R.

## 2.2. TCGA analysis

The clinical and mRNA sequencing data of The Cancer Genome Atlas Program (TCGA): Breast Invasive Carcinoma Patients– [22] was collected from cBioportal (https://www.cbioportal.org). Among the patients ($n$ = 1084), luminal breast cancer patients ($n$ = 499) were distinguished by subtype, which is clinical data. Then, using transcriptomic data from sequencing data, $PR^{Low}$ and $PR^{High}$ were categorized based on 50% with upper or lower PGR. To confirm the transcriptomic phenotype differences, PCA was conducted based on transcriptomics data using FactoMineR

package (v.2.8) fact extra package (v.1.0.7) in R. The enrichment plot was visualized to present the NES and FDR of PPP based on KEGG using gene set enrichment analysis (GSEA) (v.4.3.2).

## 2.3. Kaplan-Meier analysis

Kaplan-Meier plotter web tool was employed to visualize the survival probability of luminal breast cancer patients based on expression levels of PR and G6PD [23]. The survival probability of Q1 and Q4 was compared between patients with PR and G6PD expression, as divided into quarters. Furthermore, we compared the survival probability based on G6PD expression within each group: the low PR expression group (Q1) and the high PR expression group (Q4). To this end, the log-rank p-value and hazard ratio were calculated and presented.

## 2.4. IHC

For breast cancer patients diagnosing and subtyping, ER, PR and HER2 staining were evaluated by immunohistochemistry (IHC) using ER (1:100; clone 6F11, Novocastra), PR (1:100; clone 16, Novocastra) and HER2 (1:100; clone 4B5, Ventana Medical Systems) antibodies as previously described [24]. ER and PR status were determined by the modified Allred score and HER2 status was determined following to the American Society of Clinical Oncology (ASCO)/College of American Pathologists (CAP) guideline [25]. In accordance with the clinical data obtained, patients with hormone receptor-positive and HER2-negative were diagnosed with luminal breast cancer.

For G6PD staining, tissue microarray paraffin blocks were prepared [24], using an Accu Max Array tissue-arraying instrument (Petagen Inc.). Then, each tissue microarray slide was stained with a G6PD (1:100; NB100-236, Novus Biologicals) antibody and counterstained with hematoxylin. After staining, the cytoplasmic-G6PD expression on each slide was scored by a pathologist (Yoon-Jin Cha) using a light microscope (400× magnification). The results of IHC staining were scored as: negative 0, 1+, 2+, and 3+.

## 2.5. Cell lines and silencing PR

The MCF7 and T47D cell lines were kindly provided from the laboratory of Professor Sung Gwe Ahn. Both cell lines were cultured in RPMI 1640 (10-041-CV, Corning) supplemented with 10% fetal bovine serum (FBS; 35-015-CV, Corning) and 1% penicillin-streptomycin (15140-122, Gibco) in a humidified 5% CO2 incubator at 37 °C. Cell lines were subcultured at approximately 75%

confluence using 0.25% trypsin-EDTA (25200-072, Gibco). For PR KD, TRC-pLKO-U6 shPR lentiviral transduction particles were used to transduce both MCF7 and T47D cells. The resulting PR KD cells were selected with 1 μg/mL puromycin.

## 2.6. Real-time qPCR

RNA of the cells was extracted using TRIzol reagent (15596018, Invitrogen). And cDNA was established using ImProm-II Reverse Transcriptase (A3803, Promega). Real-time qPCR was performed using TOP Real qPCR 2X Pre-MIX (RT501S, Enzynomics) with specific primers on a CFX Connect Real-Time PCR System (1855201, Bio-Rad). Gene expression was normalized to the 36B4 as housekeeping gene using ΔΔCt method. The sequences of the primers used in the qPCR are shown below.

36B4 (F: CGTCCTCGTTGGAGTGACA, R: CGGTGCGTCAGGGATTG)

PGR (F: ACCCGCCCTATCTCAACTACC, R: AGGACACCATAATGACAGCCT)

G6PD (F: CGAGGCCGTCACCAAGAAC, R: GTAGTGGTCGATGCGGTAGA)

## 2.7. Immunoblot assay

Protein of the cells was extracted using lysis buffer (50 mM Tris-HCl, pH 8.0, 200 mM NaCl, 0.5% NP-40) with Xpert Protease Inhibitor Cocktail Solution (P3100-001, GenDEPOT). A Concentration of protein was estimated using the BCA Protein Assay kit (23227, Thermo Fisher Scientific). Equal amounts of protein were separated by sodium dodecyl sulfate polyacrylamide gel electrophoresis (SDS-PAGE) and transfer to polyvinylidene difluoride (PVDF; 162-0177, BIO-RAD). The PVDF blocked with 5% skim milk (232100, Difco) and incubated with diluted antibodies at 4 °C for overnight. Then, it was probed with horseradish peroxidase conjugated secondary antibodies. The immunoblots were visualized using enhanced chemiluminescence solution (1705061, BIO-RAD).

The primary antibodies against PR (1:2000; sc-166169, Santa Cruz Biotechnology), G6PD (1:2000; 8866S, Cell Signaling Technology), β-actin (1:5000; sc-47778, Santa Cruz Biotechnology) were used. The secondary antibodies against mouse IgG (1:10000; 7076S, Cell Signaling Technology) and rabbit IgG (1:10000; ab6721, Abcam) were used.

## 2.8. Proliferation assay

Proliferation of the cells was measured using Cell Counting Kit-8 (CCK8; CK04-13, Dojindo) according to manufacturer's instructions. In briefly, the CCK8 was treated with a volume of 1/10th the scale of the media and incubated for one hour. The absorbance was then measured in a spectrophotometer at 450 nm.

### 2.9. Bulk RNA-seq analysis

Total RNA samples were extracted and transported to Macrogen Inc. (https://www.macrogen.com) Briefly, a library was established using TruSeq Stranded mRNA Library Prep Kit (Illumina) according to manufacturer's instructions. Then, sequencing was performed by NovaSeq6000 (Illumina) platform using a NovaSeq 6000 S4 Reagent Kit (Illumina). Raw sequencing data were qualified using FastQC (v.0.11.7), trimmed using Trimmomatic (v.0.38), mapped using HISAT2 (v.2.1.0) and Bowtie2 (v2.3.4.1), and assembled using StringTie (v.2.1.3.b). Trimmed mean of M-value (TMM) normalization was conducted to normalize the read count value using edgeR package. And the DEGs were estimated using edgeR package.

### 2.10. NADPH/NADP$^+$ analysis

The ratio of NADPH/NADP$^+$ was measured using NADP/NADPH Quantitation Kit (MAK038, Sigma-Aldrich). In briefly, NADP/NADPH were extracted using extraction buffer and estimated NADPH and NADP-total value following manufacturer's instructions. The ratio of NADPH/NADP+ was calculated by ((NADPH) / (NADP-total)-(NADPH)).

## 3. RESULTS

### 3.1. scRNA-seq analysis sorting luminal epithelial cells in luminal patient data

The luminal epithelial cells and myoepithelial cells are components of breast duct system [26]. It has been suggested that the breast cancers are originated from luminal progenitors [27-31]. In contrast, the myoepithelial cells serve as a barrier to the invasion and dissemination of luminal epithelial cancer cells [32]. To investigate the relation of PR, PPP and aggressiveness in luminal

breast cancer, we performed scRNA-seq analysis using published data from the Gene Expression Omnibus (GEO) database (**Fig. 1A**).

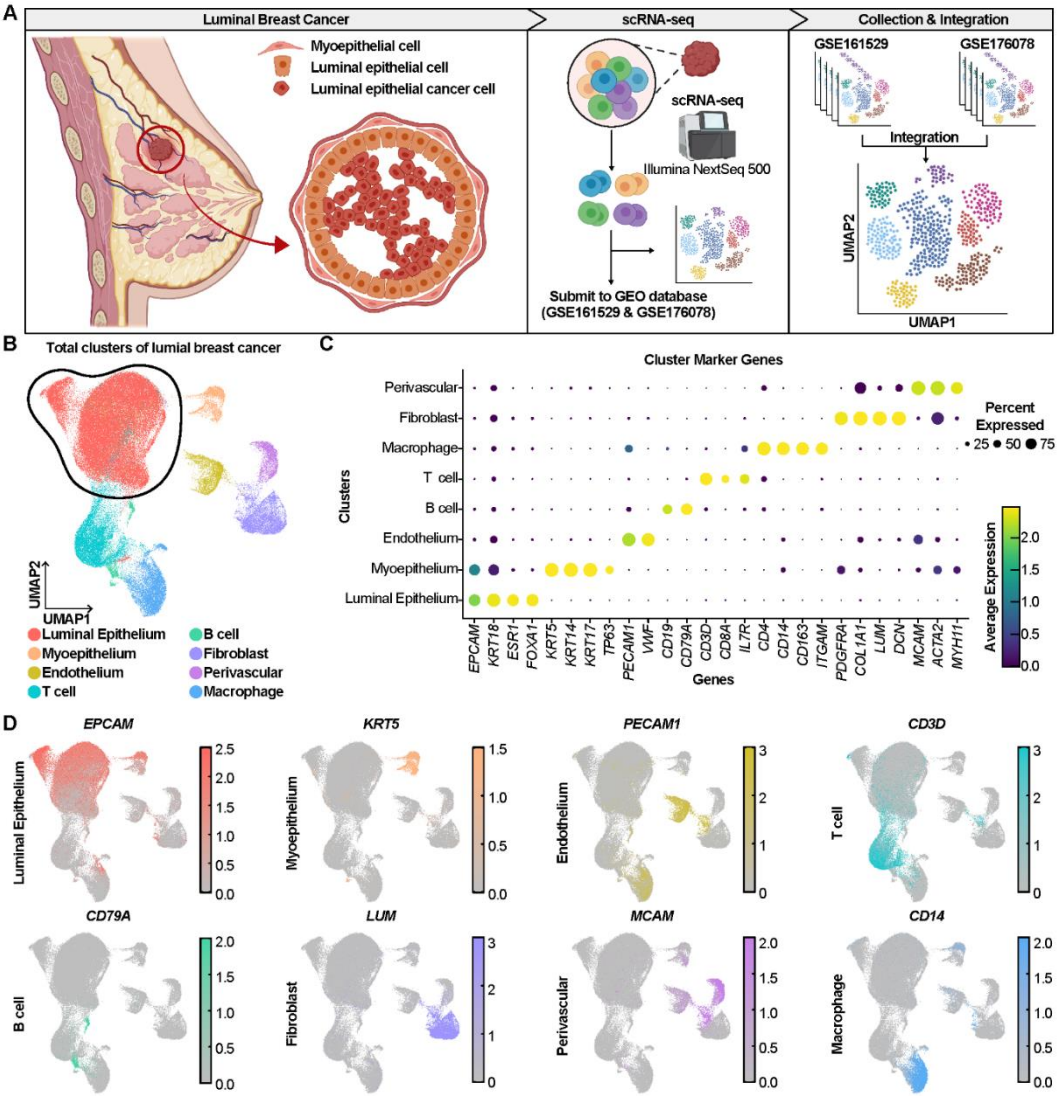


**Fig. 1 scRNA-seq analysis categorizing eight cell types in luminal breast cancer patient data.** **A** The luminal breast cancer is primarily caused by excessive growth of the aggressive luminal epithelial cell surrounded by myoepithelial cells. **B** Dimension plot presenting identified eight different cell types. **C-D** Dot plot and feature plot showing marker genes of cell types.

First, we collected 33 luminal patient matrices of scRNA-seq data based on the 10x Genomics platform from GSE161529 [19] and GSE176078 [20]. These matrices were processed using Seurat package in R. Through the process of quality control and integration, approximately 100,000 cells were used in analysis.

Then, to visualize these cells on two-dimension using uniform manifold approximation and projection (UMAP), principal component analysis (PCA) was performed (**Fig. 1B**). It presented that about 100,000 cells were divided into eight clusters and these clusters had distinctive identities of characteristic lineage cell with marker genes. These include *EPCAM*, *KRT18*, *ESR1*, *FOXA1* for luminal epithelial cell, *KRT5*, *KRT14*, *KRT17*, *TP63* for myoepithelial cell, *PEACAM1*, *VWF* for endothelium, *CD3D*, *CD8A*, *IL7A* for T cell, *CD19*, *CD79A* for B cell, *PDGFRA*, *COL1A1*, *LUM*, *DCN* for fibroblasts, *MCAM*, *ACTA2*, *MYH11* for perivascular cell, and *CD4*, *CD14*, *CD163*, *ITGAM* for macrophage, as observed across different clusters (**Fig. 1C-D**). Among eight cell types, the luminal epithelial cell cluster, which is the dominant cancer cell in luminal breast cancer [27-31], was subset (**Supplementary Fig. 1A**).

Then, to visualize these cells on two-dimension using uniform manifold approximation and projection (UMAP), principal component analysis (PCA) was performed (**Fig. 1B**). It presented that about 100,000 cells were divided into eight clusters and these clusters had distinctive identities of characteristic lineage cell with marker genes. These include *EPCAM*, *KRT18*, *ESR1*, *FOXA1* for luminal epithelial cell, *KRT5*, *KRT14*, *KRT17*, *TP63* for myoepithelial cell, *PEACAM1*, *VWF* for endothelium, *CD3D*, *CD8A*, *IL7A* for T cell, *CD19*, *CD79A* for B cell, *PDGFRA*, *COL1A1*, *LUM*, *DCN* for fibroblasts, *MCAM*, *ACTA2*, *MYH11* for perivascular cell, and *CD4*, *CD14*, *CD163*, *ITGAM* for macrophage, as observed across different clusters (**Fig. 1C-D**). Among eight cell types, the luminal epithelial cell cluster, which is the dominant cancer cell in luminal breast cancer (Adriance et al., 2005; Prat & Perou, 2009; Molyneux et al., 2010; Proia et al., 2011; Keller et al., 2012), was subset (**Supplementary Fig. 1A**).

## 3.2. Luminal epithelial cells divided by cell cycle rate and PR expression

The most interesting aspect of the luminal epithelial cell subcluster was its positioning within a right-sided island (black dotted line), as illustrated in the UMAP (**Fig. 2A**). This island part showed

significantly increased proliferation marker genes, *MKI67* [33] and *TOP2A* [34] (**Fig. 2B**). In addition, the island part exhibited that elevated 'E2F Targets' score based on Hallmark database [35] using GSEA [36] (**Fig. 2B**). The serial data demonstrated that the island cells were proliferative, leading that these island cells designated as Cycling group and the rest of the cells as NC group (non-cycling). To confirm the Cycling group was undergoing proliferation, cell cycle phase analysis was conducted. It revealed that the Cycling group exhibited a much higher percentage of G2M (72.3 %) phases than NC (26.1%) (**Fig. 2C**). Therefore, these proliferative cells were regarded as representative of malignant luminal epithelial cells.

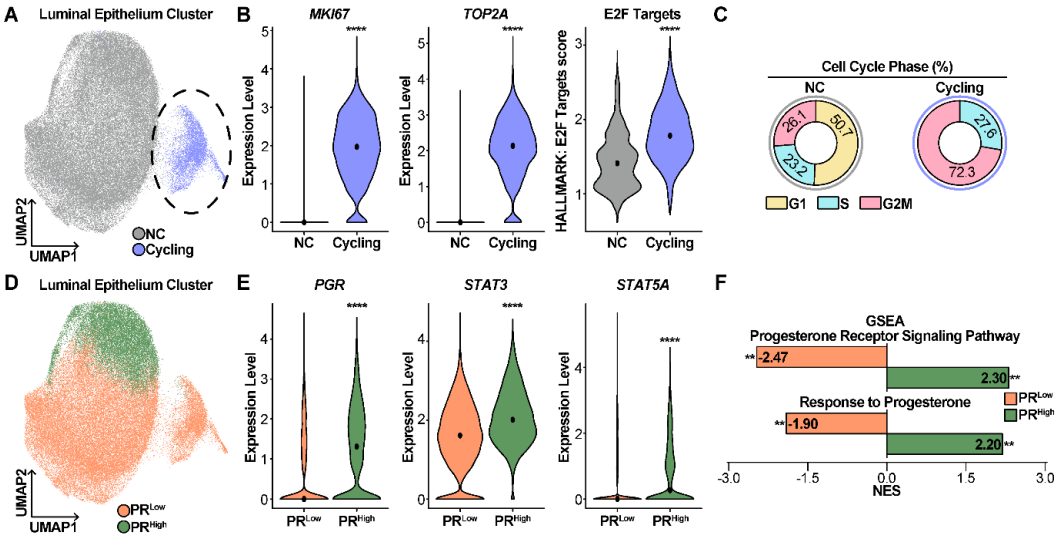


**Fig. 2 A division of luminal epithelial cells based on proliferation and PR expression. A** Dimension plot displaying of NC and Cycling groups. **B** Violin plots presenting expression levels of *MKI67* and *TOP2A*, and score of E2F targets. **C** Cell cycle phase ratio of NC and Cycling groups. **D** Dimension plot exhibiting PR $^{low}$ and PR $^{high}$ groups. **E** Violin plot showing expression levels of *PGR*, *STAT3*, and *STAT5A*. **F** Bar plot exhibiting NES of progesterone related pathways. The violin plots of **B** and **E** were presented as median expression value with adjusted *p* value. **** $p < 0.0001$.

Interestingly, the luminal epithelial cell cluster also could be separated by *PGR* expression (**Fig. 2D**), leading to two distinct groups, PR $^{Low}$ group and PR $^{High}$ group. As expected, the PR $^{Low}$ group exhibited statistically lower expression of *PGR* than the PR $^{High}$ group. And direct target genes of

PR [37], *STAT3* and *STAT5A*, were significantly diminished in the PR $^{Low}$ group (**Fig. 2E**). In addition, PR $^{Low}$ group carried with negative NES of Progesterone Receptor Signaling Pathway (NES = -2.47) and Response to Progesterone (NES = -1.90) based on KEGG database using GSEA [38] (**Fig. 2F**). This data demonstrated that PR $^{Low}$ group had down-regulated activity of PR related signaling. Also, the cluster divisions based on a proliferation and PR were an optimal analytical model for the aggressiveness of luminal breast cancer according to PR expression.

## 3.3. Proliferative luminal epithelial cells with PR $^{Low}$ exhibiting upper PPP activity and G6PD expression

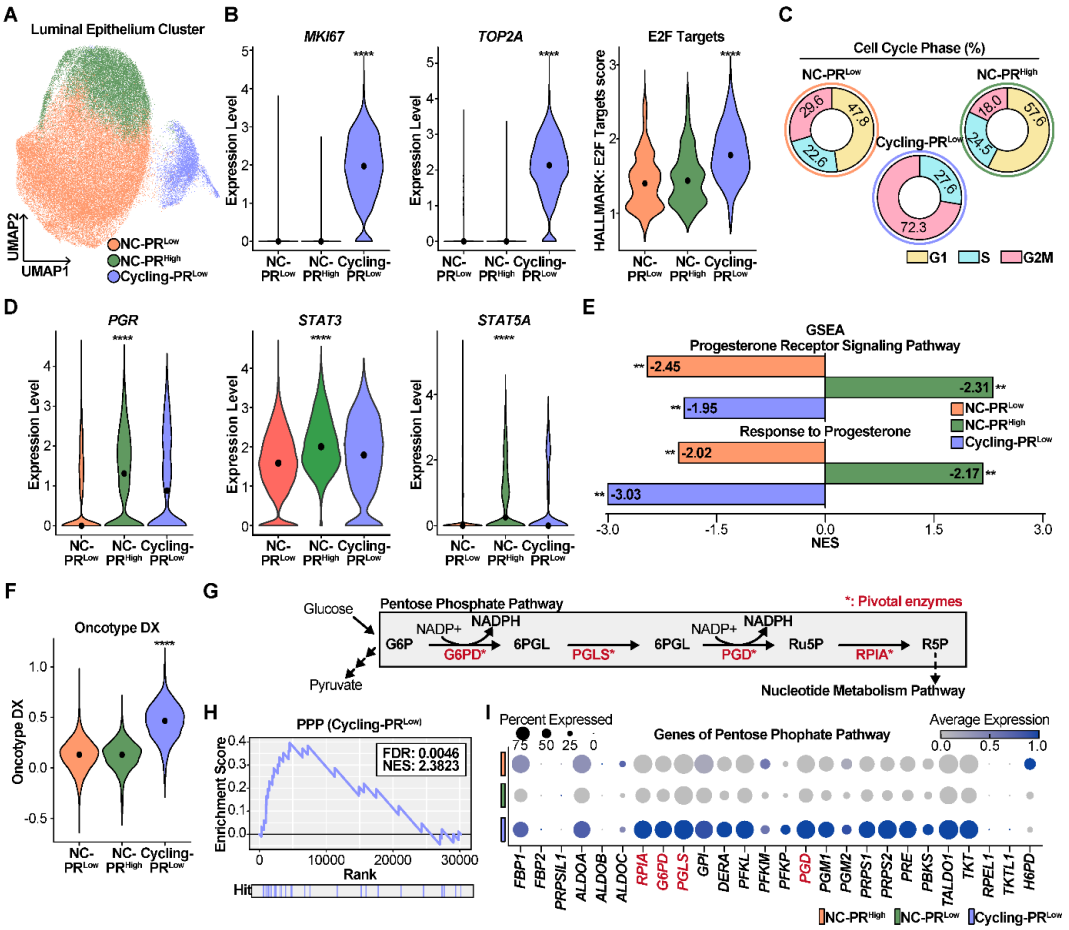

**Fig. 3 Cycling-PR $^{low}$ epithelial cells revealing high PPP activity and G6PD expression. A** Dimension plot displaying NC-PR $^{low}$, NC-PR $^{high}$, and Cycling-PR $^{low}$ groups. **B-C** Violin plots presenting expression levels of *MKI67*, *TOP2A*, *PGR*, and *STAT5A*, and score of E2F targets. **D** Cell cycle phase ratio of three subclusters. **E** Bar plot showing NES of progesterone related pathways. **F** Violin plot exhibiting Oncotype DX. **G** Schematic model of PPP. **H** Enrichment plot of PPP. The highlighted genes, G6PD, PGLS, PGD, and RPIA~~,~~ are directly control metabolites of PPP. **I** Dot plot showing genes included in PPP gene set. The violin plots of **B**, **D**, and **F** were presented as median expression value with adjusted *p* value. **** $p < 0.0001$.

An intriguing phenomenon was found that all cells in the Cycling group belonged to the PR $^{Low}$ group (**Fig. 2A and 2D**). To further analyze this, three categorized cell clusters were designated as NC-PR $^{Low}$, NC-PR $^{High}$ and Cycling-PR $^{Low}$ groups (**Supplementary Fig. 1B, Fig. 3A**). Cycling-PR $^{Low}$ cluster maintained their proliferative characteristics (**Fig. 3B-C**), while exhibiting low expression of *PGR*, *STAT3* and *STAT5A*, as well as negative NES of progesterone-related signaling compared to NC-PR $^{High}$ (**Fig. 3D-E**). These finds indicated that Cycling-PR $^{Low}$ cells were aggressive and had low PR activity.

The most interesting observation was that RS of 21-multigene assay [8, 9], which predicts the recurrence and aggressiveness of breast cancer, was significantly elevated in the Cycling-PR $^{Low}$ cluster (**Fig. 3F**). In contrast, the disparity of RS between the NC-PR $^{Low}$ and NC-PR $^{High}$ was too minimal to have a significant foldchange (**Fig. 3F**).

To investigate the lack evidence for an inverse relation of PR and PPP, subclusters were analyzed with a focus on PPP. PPP functions through pivotal enzymes, including G6PD and PGD, which form NADPH, as well as PGLS and RPIA, which also directly interact with metabolites [14] (**Fig. 3G**). To analyze these pivotal enzymes, the PPP gene set from the KEGG pathway was used. The Cycling-PR $^{Low}$ group exhibited significantly increased PPP activity, with positive NES of 2.3823 and FDR of 0.0046 (**Fig. 3H**). Furthermore, the expression of genes in the PPP gene set was elevated in the Cycling-PR $^{Low}$ group (**Fig. 3I**). Among these, the pivotal enzymes were significantly up-regulated in Cycling-PR $^{Low}$ group (**Supplementary Fig. 1C**). scRNA-seq analysis conducted thus far demonstrated that aggressive cells with low PR expression had increased PPP activity and elevated G6PD expression.

To further validate the findings, additional analysis was conducted using the copy number variation score. The CopyKAT package [39] in R was utilized to classify the epithelial cluster into aneuploid, diploid, and undefined cells (**Supplementary Fig. 2A**). Aneuploid cells, which exhibited an abnormal number of chromosomes with high CNV score, were subsetted (**Supplementary Fig. 2B**). These aneuploid cells were then divided into NC-PR $^{Low}$, NC-PR $^{High}$, and Cycling-PR $^{Low}$ groups for further analysis. Similar patterns in PR and G6PD expression, as well as RS of 21-multigene assay and PPP scores, were observed, consistent with the previous results (**Supplementary Fig. 2C**).

## 3.4. Clinical implication of reverse association between PR and G6PD in luminal patients

To study linkage between G6PD and PR expression in luminal breast cancer patients, data from TCGA: Breast Invasive Carcinoma Patients [22] was used. There are 1,084 breast cancer patients, with 696 luminal breast cancer patients included in the study. The luminal breast cancer patients were divided into two groups, PR $^{Low}$ ($n$ = 200) and PR $^{High}$ ($n$ = 200), based on their *PGR* expression level (**Fig. 4A**). The group division was confirmed with a visualization of *PGR* expression (**Fig. 4B**). Interestingly, the groups divided solely by *PGR* expression exhibited transcriptomic phenotypic differences (**Fig. 4C**). In addition, PR $^{Low}$ patients showed significantly up-regulated PPP activity (NES = 0.00317 and FDR = 0.0317) (**Fig. 4D**). And the expression level of *G6PD*, *PGLS*, *PGD*, and *RPIA*, pivotal enzymes of PPP (**Fig. 3G**), were increased in PR $^{Low}$ patients with statistical significance (**Fig. 4E**). KEGG analysis of clinical data suggested that patients with low PR expression were characterized by enriched PPP and elevated G6PD expression.

Here, we presented those 72 patients' data diagnosed with luminal breast cancer with clinical PR status and intensity score of G6PD using IHC. The 72 patients were divided into PR $^{Low}$ ($n$ = 18), PR $^{High}$ ($n$ = 54) based on PR status, and they were split into G6PD $^{Low}$ ($n$ = 46), G6PD $^{High}$ ($n$ = 26) based on G6PD score (**Fig. 4F-G, Supplementary Fig. 3A-D**). It showed that a larger proportion (61 %) of patients with PR $^{Low}$ exhibited higher G6PD expression, while a larger proportion (72 %) of patients with PR $^{High}$ exhibited lower G6PD expression with significance ($p$ = 0.011) (**Fig. 4F**). 72 luminal breast cancer patients' data demonstrated a significant negative correlation between G6PD and PR.

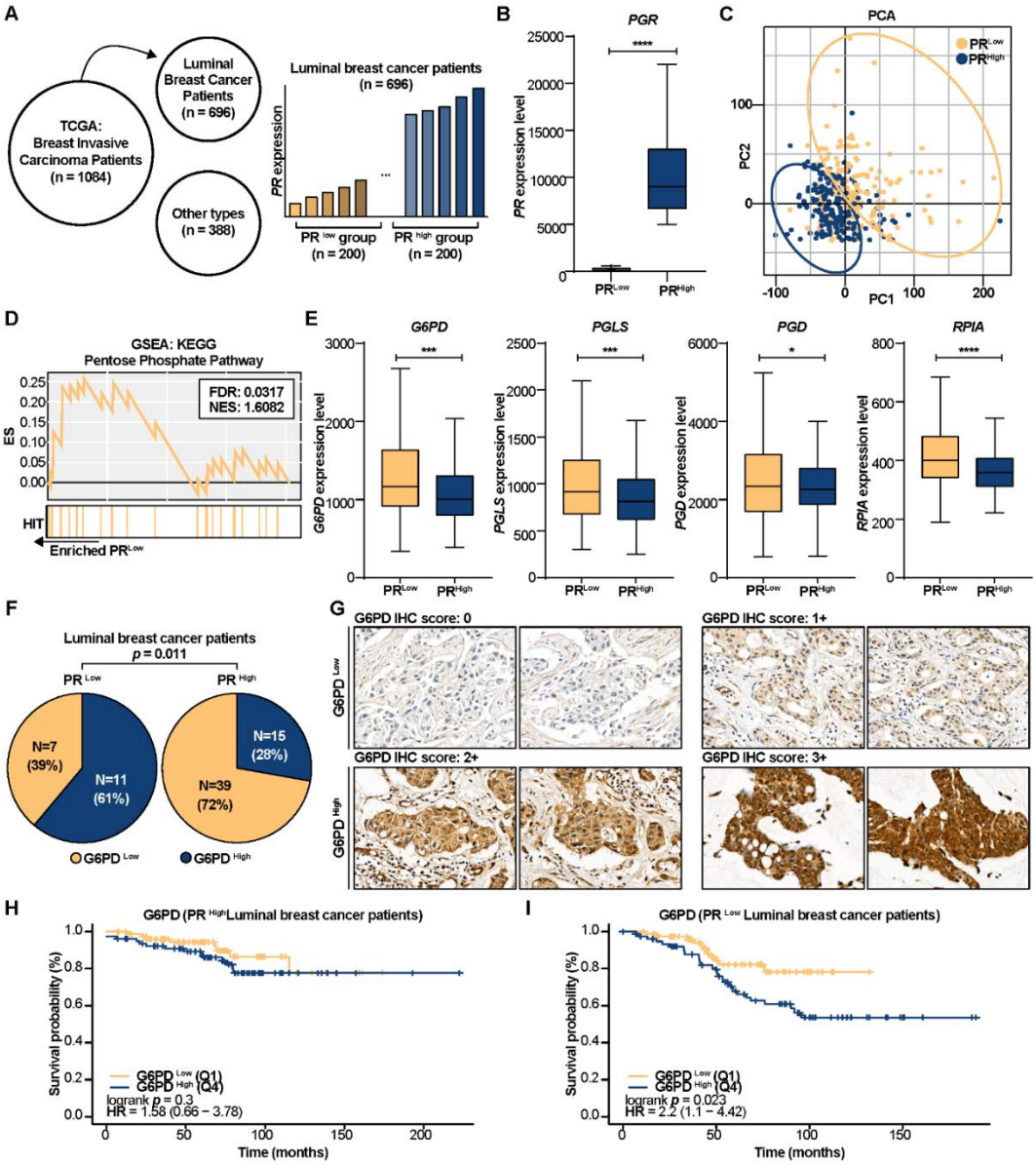


**Fig. 4. Clinical implication of luminal breast cancer patients representing inverse relation between PR and G6PD. A** Scheme of analysis of breast invasive carcinoma patients from TCGA and division patients based on PR expression. **B** Box plot presenting the expression levels of PR in the PR $^{low}$ and PR $^{high}$ groups. **C** PCA plot displaying the proportion between PR $^{low}$ and PR $^{high}$ groups. **D** Enrichment plot of PPP enriched in the PR $^{low}$ group. **E** Box plots showing the expression

levels of key metabolic intermediating enzymes, *G6PD*, *PGLS*, *PGD*, and *RPIA*. **F** Ratio of the PR $^{low}$ and PR $^{high}$ patients within G6PD $^{low}$ and G6PD $^{high}$ patients from Severance hospital. **G** IHC of luminal breast cancer patients presenting protein expression of G6PD (magnification × 400) from Severance hospital. **H and I** Kaplan–Meier plots comparing survival probabilities based on G6PD expression in luminal breast cancer patients with low or high PR expression, generated using the Kaplan–Meier plotter tool. For **E**, mean value was marked as + in box plots. For **B** and **E**, all data were presented as mean value with standard deviation and unpaired *t*-test. $p < 0.0001$. * $p < 0.05$, *** $p < 0.001$, **** $p < 0.0001$.

To ascertain the survival probabilities of luminal breast cancer patients associated with PR and G6PD expression, the Kaplan-Meier plotter web tool was employed [23]. The patients were divided into PR $^{Low}$ (quartiles; Q1) and PR $^{High}$ (Q4) groups based on PR expression. They showed PR $^{High}$ (Q4) group was significantly higher probability ($p = 0.0000$) with hazard ratio of 0.52 compared to PR $^{Low}$ (**Supplementary Fig. 4A**). On the other hand, G6PD $^{High}$ (Q4) was significantly lower probability ($p = 0.0001$) with hazard ratio of 1.43 compared to G6PD $^{Low}$ (**Supplementary Fig. 4B**). Importantly, no statistically significant difference in survival probability was observed among PR $^{High}$ patients based on G6PD expression levels ($p = 0.3$) (**Fig. 4H**). In contrast, among PR $^{Low}$ patients, higher G6PD expression was associated with significantly lower survival probability ($p = 0.023$) (**Fig. 4I**). These results suggest that the impact of G6PD expression on survival may be greater in patients with low PR expression. The KEGG analysis, clinical luminal breast cancer patient analysis, and Kaplan-Meier analysis all strongly demonstrated that PR would be clinically associated with PPP and G6PD, which affected the survival rate of luminal breast cancer patients.

## 3.5. Aggressiveness induction through silencing PR on LA breast cancer cell lines

The relationship between PR and G6PD established by scRNA-seq analysis and clinical data analysis led to PR KD on the luminal breast cancer cell lines. Two luminal breast cancer cell lines, MCF7 and T47D, were employed [40, 41] and lentiviral vectors were used to silence *PGR* expression (**Fig. 5A**). The PR reduction of PR KD cell lines (shPR) and was confirmed by quantitative polymerase chain reaction (qPCR) and immunoblotting compared to control cell lines (shNS) (**Fig. 5B-C**).

Subsequently, the proliferation rate of the shNS and shPR was estimated to evaluate the aggressiveness difference. The proliferation rate of shPR was statistically elevated compared to shNS (**Fig. 5D**). Importantly, the growth rate at 72h was increased both shPR-MCF7 (p = 0.0002) and shPR-T47D ($p$ = 0.0071) (**Fig. 5D**). In breast cancer cells, factors that increase cancer proliferation imply a risk of high tumor grade, metastasis, and death induction in patients [42-45], suggesting that malignancy induced to shPR cells.

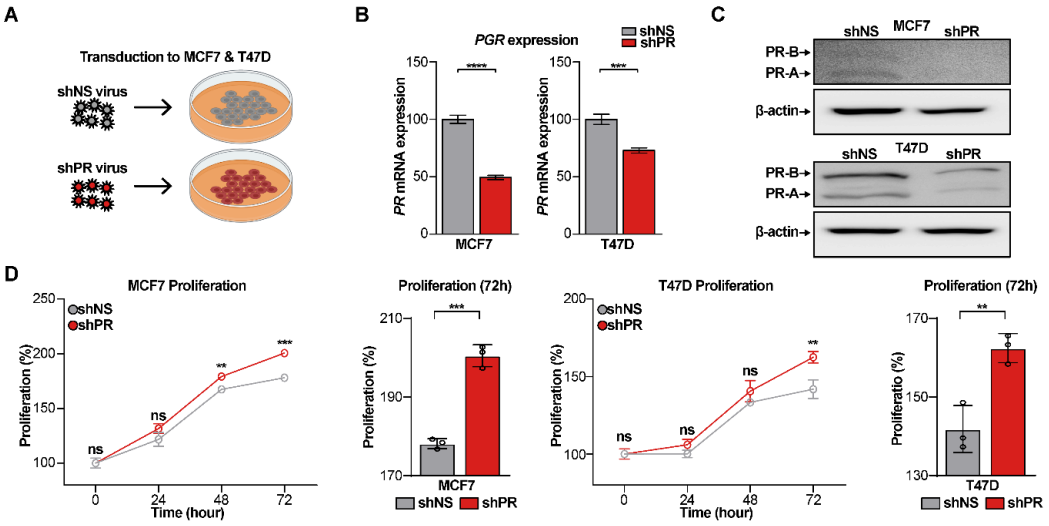


**Fig 5. Increased proliferation rate of PR KD breast cancer cell lines. A** Schemic model illustrating transduction of lentiviral particles to the breast cancer cell lines, MCF7 and T47D. **B-C** Bar plot and western blot presenting mRNA and protein expression of PR. **D** Proliferation rate of shPR and shNS groups exhibiting a faster growth of PR KD cell lines. The proliferation ratio at 72 h showing a statistically significant improvement in PR KD cell lines. For **B** and **D**, all data were presented as mean value with standard deviation and unpaired $t$-test. ** $p < 0.01$, *** $p < 0.001$, **** $p < 0.0001$.

## 3.6. Bulk RNA-seq analysis showed increased PPP activity in PR KD cell lines

To research the features of aggressiveness induced by PR KD in both cell lines, bulk RNA-seq was conducted. Sequencing was performed on Illumina NovaSeq 6000 platform system comparing

shNS and shPR (**Fig. 6A**). First, *PR* expression was assessed using normalized expression values in TPM (**Supplementary Fig. 5A**). In addition, *ESR* expression, a key target of tamoxifen [46], was also evaluated. In MCF7 cells, no significant p-value was obtained, and in T47D cells, the observed fold change of -1.1 was not meaningful, showing no substantial difference between the two groups. (**Supplementary Fig. 5A**). Then, differentially expressed genes (DEGs) analysis was performed to identify genes with significant expression differences between the two groups Genes showing a two-fold change in expression between shNS and shPR, with a p-value of less than 0.05, were designated as DEGs. A total of 39 up-regulated and 14 down-regulated genes were identified as shared DEGs between the two cell lines (**Supplementary Fig. 5B-D**). Nevertheless, the 53 shared DEGs were insufficient for the purposes of enrichment analysis, necessitating GSEA using total gene expression.

GSEA based on KEGG carried out that positive NES of "Glycolysis Gluconeogenesis", "Fructose and Mannose Metabolism", and "Pentose Phosphate Pathway", and negative NES of "Oxidative Phosphorylation" (OXPHOS) in both PR KD cell lines (**Fig. 6B-C**). The OXPHOS reduction leading impaired ATP production could be interpreted as an increased utilization of glucose, fructose and mannose in PR KD breast cancer cells.

The most important aspect of GSEA results was the ascending of the PPP in both MCF7 (NES = 1.51, $p = 0.045$) and T47D (NES = 1.51, $p = 0.042$) (**Fig. 6D**). An increase in glucose utilization would have resulted in an elevation of PPP, which represents the shunt pathway of glycolysis. The shared core genes of the PPP were evaluated to *ALDOA*, *G6PD*, *FBP1*, *TKT*, and *PFKP* (**Fig. 6E**). Among the shared core genes, there was only one, *G6PD*, the pivotal enzyme.

To gain insight into the intracellular mechanisms underlying the PPP, we used the Enrichment Map application [47] based on gene ontology: biological process (GOBP) [48]. The enrichment map result was processed with *p*-value cutoff ($p < 0.05$), annotated using the AutoAnnote application [49], and visualized using Cytoscape [50]. The Enrichment map result showed that PR KD led to a decrease in OXPHOS and an increase in glycolysis consistent with GSEA-KEGG analysis (**Fig. 6F**). It postulated that the observed increase in glycolysis could be potentiated by the utilization of the G6PD-mediated pathway (**Fig. 6F**).

## 3.7. Aggressiveness of PR KD cells impeded by G6PDi.

To validate the bulk RNA-seq analysis results at the cellular level, we confirmed the increased G6PD expression at the mRNA and protein level (**Fig. 7A-B**). Given that G6PD functions for

NADPH production [14], the significantly increased ratio of NADPH/NADP$^+$ observed in the PR KD cells (**Fig. 7C**). The elevated NADPH/NADP$^+$ ratio demonstrated that PR KD cells increased PPP in vitro.

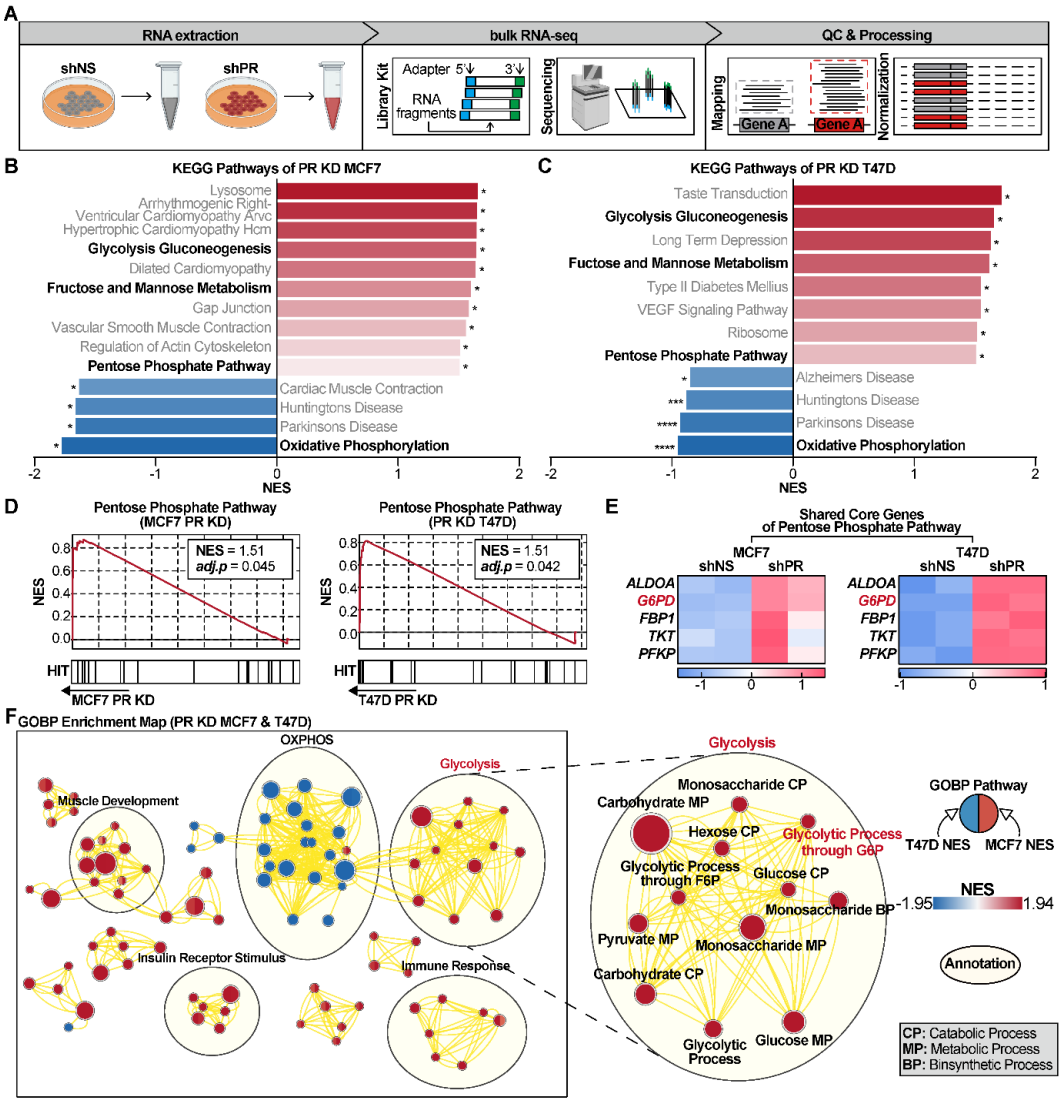


**Fig. 6 Bulk RNA-seq analysis presenting elevated PPP activity in PR KD cell lines. A** Schemic graphic of bulk RNA-seq processing to identify differences of phenotype between shNS and shPR. **B-C** Bar plots of statistically significant KEGG pathway lists marked with crucial shared pathways,

presenting up-regulated PPP activity in PR KD cell lines. **D** The enrichment plot of PPP in PR KD cell lines. **E** Heatmaps displaying shared core genes of PPP. **F** Enrichment map visualizing results of GO BP in PR KD cell lines. The map demonstrated that positive NES of "Glycolytic Process through G6P" was observed. * $p < 0.05$, **** $p < 0.0001$.

To inhibit the increased function of PPP by G6PD, the chemical that selectively inhibits G6PD, G6PDi, was utilized in this study. G6PDi inhibits the PPP and depletes NADPH of cells [18]. The proliferation assay using 20μM G6PDi showed a plunge of cell growth rate of shPR + G6PDi group than shNS + Vehicle and shPR + Vehicle groups (**Fig. 7D**). Specifically, the proliferation rate at 72h presented shPR + G6PDi group was decreased both MCF7 and T47D ($p < 0.0001$) compared to other groups (**Fig. 7D**). These findings demonstrated that the aggressiveness of PR KD cancer cells was diminished by inhibiting G6PD.

Interestingly, efficacy was noted when G6PDi was combined with tamoxifen, a widely used therapeutic agent for luminal breast cancer (**Supplementary Fig. 6A**). A greater reduction in proliferation was observed in the combination assay with 1 μM tamoxifen and 20 μM G6PDi compared to the effects of each drug individually. These results suggest a potential synergistic interaction between tamoxifen and G6PDi, highlighting the combination as a promising therapeutic strategy for luminal breast cancer.

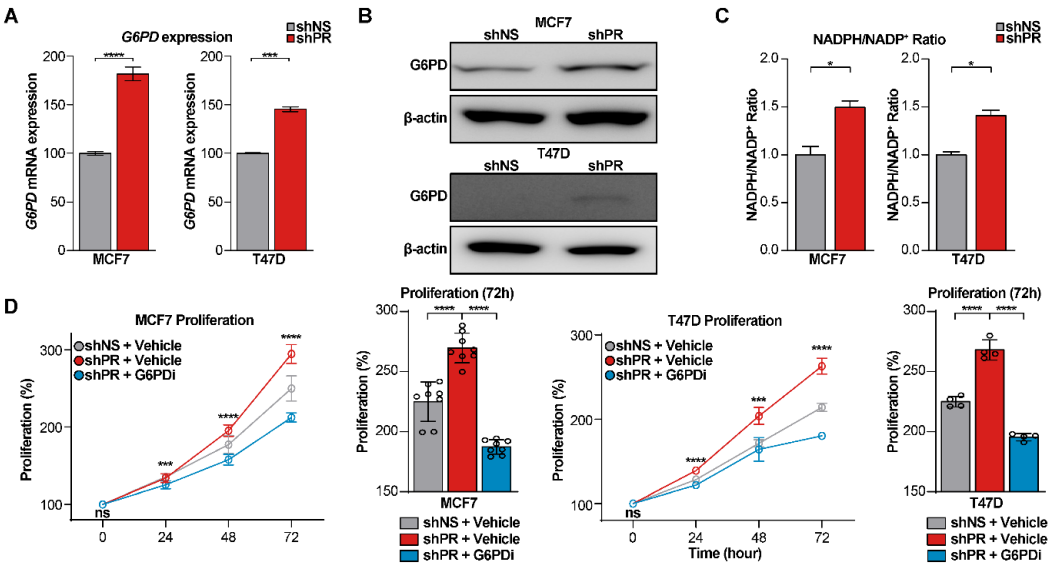

**Fig. 7. G6PDi, selective inhibitor of G6PD, reduced aggressiveness of the PR KD. A-B** Bar plot and western blot presenting mRNA and protein expression of G6PD. **C** Bar graph showing the ratio of NADPH/$NAP^+$ between shNS and shPR. **D** Proliferation rate of three groups, shNS with vehicle, shPR with vehicle, and shPR with G6PDi. The proliferation ratio at 72 h presented reduction of cell growth in shPR + G6PDi. Bar graphs of **A, C** and **D** were presented as mean values with standard deviation and unpaired *t*-test *p* value. The proliferation plots of **D** were presented as mean value with standard deviation and one-way ANOVA. * $p < 0.05$, *** $p < 0.001$, **** $p < 0.0001$.

# 4. DISCUSSION

Our series of experiments demonstrated that glucose metabolism, including the PPP and related enzymes, is activated in luminal breast cancer with low PR expression. Moreover, we were able to confirm that the inhibition of G6PD, a key enzyme of the PPP, could suppress the aggressiveness of low PR tumors. This suggests that the inhibition of glucose metabolism, including G6PDi, could be a new therapeutic strategy utilizing PR as a biomarker in the future.

PR is essential for regulating the activity of estrogen receptors α (ERα) in breast cancer [51]. As an upregulated target gene of ER, PR expression is largely dependent on estrogen levels. The mechanism regarding the prognostic effect of PR in breast cancer are subject to various opinions. Previous study has suggested that PR directly inhibit estrogen-induced tumor growth by translocating ER from mitotic sites to apoptosis and cell death genes [52]. Additionally, another study claimed that PR regulated overall tumor growth by modulating RNA polymerase III [53]. It was also reported that ER-positive/PR-negative breast cancer exhibits upregulation of PI3K/Akt/mTOR pathway activity compared to PR-positive luminal breast cancer [54]. On the other hand, based on our previous clinical studies [10, 11], we focused on the association between PR and glucose metabolism, and we were able to obtain largely positive results.

To study the significance of PR expression in luminal breast cancer, we performed scRNA-seq analysis using a published patient dataset. We found that in certain luminal epithelial cells, low PR expression with faster proliferative luminal epithelial cells were associated with increased PPP activity and increased G6PD expression. These findings indicated that proliferative cells with lower PR expression might be associated with increased PPP activity following NADPH needs, suggesting metabolic shift based on PR expression. G6PD, the first enzyme in the PPP, plays a critical role in

producing NADPH, which is essential for oxidative stress management and cellular metabolism. The correlation between low PR expression and increased G6PD activity suggests that metabolic reprogramming may drive the aggressiveness of these luminal epithelial cells. This highlighted the potential aggressiveness of the cycling PR $^{Low}$ cluster and suggested that G6PD might be a potential therapeutic target for aggressive luminal epithelial breast cancer cells.

To verify the clinical implications of our scRNA-seq analysis results, we devised and conducted analyses using various methods, including TCGA dataset, tumor tissue samples derived from breast cancer patients, and the Kaplan-Meier plotter web tool. As a result, through multiple analyses, we confirmed that not only the PPP and G6PD expression activated in low PR tumors, but this activation also affected the survival outcomes of luminal breast cancer patients.

Given the reports that higher G6PD expression levels are associated with a higher hazard ratio in breast cancer patients, we hypothesized that PR expression might directly influence luminal breast cancer in association with G6PD. MCF7 and T47D cells were transduced with PR-targeting shRNA constructs, and silencing efficiency was confirmed through Western blot analysis. Control cells were transduced with non-targeting shRNA. These PR KD cell lines exhibited faster proliferation rates, increased PPP activity, and increased G6PD expression than control cells.

Treatment with the G6PD inhibitor, G6PDi, significantly reduced the proliferation of PR KD cells compared to control cells. This supports a functional link between PR expressions and G6PD-driven metabolic reprogramming. The observed reduction in proliferation highlights the potential of G6PD as a therapeutic target, especially in aggressive PR-low luminal breast cancer cells. These results provide important information for understanding the interaction between PR and G6PD and suggest a new approach for the treatment of aggressive luminal breast cancer.

With our knowledge, our study is the first to experimentally demonstrate the correlation between PR and G6PD. Increased expression of G6PD has been observed in various cancers, including renal cell carcinoma, gastric cancer, and bladder cancer [55-57]. It has been also reported that G6PD expression negatively impacts metastasis and prognosis in breast cancer. However, these studies did not link PPP, including G6PD, to PR expression, whereas our research identified the association between G6PD and PR expression.

G6PD inhibitors have not yet been used in the treatment of malignant tumors in clinical practice, but research on the use of G6PD inhibitors in ongoing for various cancers such as ovarian cancer and tongue cancer [58, 59]. Our study also confirmed the potential therapeutic effects of G6PD

inhibitors in luminal breast cancer and demonstrated that PR expression could be used as a biomarker for the administration of G6PD inhibitors.

The limitation of our study is that all experiments were performed exclusively *in vitro* using PR KD cell lines, which do not fully capture the complexity of the tumor microenvironment or the physiological conditions found *in vivo*. Furthermore, the absence of in vivo validation through animal models limits the ability to confirm the efficacy and safety of the G6PDi therapy in more complex biological systems. As a result, the translational potential of our findings to clinical practice remains uncertain.

# 5. CONCLUSION

We presented a treatment strategy for identification and validation of luminal breast cancer through selection of candidate genes based on genomic analysis and biological analysis. We identified that the aggressiveness of low PR tumors is associated with the PPP and its key enzyme, G6PD. Moreover, G6PDi has suggested the potential for a new therapeutic drug in luminal breast cancer, using PR as a biomarker.

# REFERENCES

1. Sørlie T. Molecular portraits of breast cancer: tumour subtypes as distinct disease entities. European journal of cancer. 2004;40:2667-75.
2. Zubair M, Wang S, Ali N. Advanced Approaches to Breast Cancer Classification and Diagnosis. Front Pharmacol. 2020;11:632079.
3. Dieleman S, Aarnoutse R, Ziemons J, Kooreman L, Boleij A, Smidt M. Exploring the Potential of Breast Microbiota as Biomarker for Breast Cancer and Therapeutic Response. Am J Pathol. 2021;191:968-82.
4. Pandit P, Patil R, Palwe V, Gandhe S, Patil R, Nagarkar R. Prevalence of Molecular Subtypes of Breast Cancer: A Single Institutional Experience of 2062 Patients. Eur J Breast Health. 2020;16:39-43.
5. Poudel P, Nyamundanda G, Patil Y, Cheang MCU, Sadanandam A. Heterocellular gene signatures reveal luminal-A breast cancer heterogeneity and differential therapeutic responses. NPJ Breast Cancer. 2019;5:21.
6. Van Asten K, Slembrouck L, Olbrecht S, Jongen L, Brouckaert O, Wildiers H, et al. Prognostic Value of the Progesterone Receptor by Subtype in Patients with Estrogen Receptor-Positive, HER-2 Negative Breast Cancer. Oncologist. 2019;24:165-71.
7. Luo Y, Li Q, Fang J, Pan C, Zhang L, Xu X, et al. ER+/PR- phenotype exhibits more aggressive biological features and worse outcome compared with ER+/PR+ phenotype in HER2-negative inflammatory breast cancer. Sci Rep. 2024;14:197.
8. Tang P, Wang J, Hicks DG, Wang X, Schiffhauer L, McMahon L, et al. A lower Allred score for progesterone receptor is strongly associated with a higher recurrence score of 21-gene assay in breast cancer. Cancer Invest. 2010;28:978-82.
9. Huang JL, Kizy S, Marmor S, Altman A, Blaes A, Beckwith H, et al. Tumor grade and progesterone receptor status predict 21-gene recurrence score in early stage invasive breast carcinoma. Breast Cancer Res Treat. 2018;172:671-7.
10. Ahn SG, Lee JH, Lee HW, Jeon TJ, Ryu YH, Kim KM, et al. Comparison of standardized uptake value of 18F-FDG-PET-CT with 21-gene recurrence score in estrogen receptor-positive, HER2-negative breast cancer. PLoS One. 2017;12:e0175048.

11. Ahn SG, Yoon CI, Lee JH, Lee HS, Park SE, Cha YJ, et al. Low PR in ER(+)/HER2(-) breast cancer: high rates of TP53 mutation and high SUV. Endocr Relat Cancer. 2019;26:177-85.
12. Ahn SG, Lee M, Jeon TJ, Han K, Lee HM, Lee SA, et al. [18F]-fluorodeoxyglucose positron emission tomography can contribute to discriminate patients with poor prognosis in hormone receptor-positive breast cancer. PLoS One. 2014;9:e105905.
13. Alfarouk KO, Verduzco D, Rauch C, Muddathir AK, Adil HB, Elhassan GO, et al. Glycolysis, tumor metabolism, cancer growth and dissemination. A new pH-based etiopathogenic perspective and therapeutic approach to an old cancer question. Oncoscience. 2014;1:777.
14. Ge T, Yang J, Zhou S, Wang Y, Li Y, Tong X. The Role of the Pentose Phosphate Pathway in Diabetes and Cancer. Front Endocrinol (Lausanne). 2020;11:365.
15. Riganti C, Gazzano E, Polimeni M, Aldieri E, Ghigo D. The pentose phosphate pathway: an antioxidant defense and a crossroad in tumor cell fate. Free Radic Biol Med. 2012;53:421-36.
16. Pu H, Zhang Q, Zhao C, Shi L, Wang Y, Wang J, et al. Overexpression of G6PD is associated with high risks of recurrent metastasis and poor progression-free survival in primary breast carcinoma. World J Surg Oncol. 2015;13:323.
17. Choi J, Kim ES, Koo JS. Expression of Pentose Phosphate Pathway-Related Proteins in Breast Cancer. Dis Markers. 2018;2018:9369358.
18. Ghergurovich JM, Garcia-Canaveras JC, Wang J, Schmidt E, Zhang Z, TeSlaa T, et al. A small molecule G6PD inhibitor reveals immune dependence on pentose phosphate pathway. Nat Chem Biol. 2020;16:731-9.
19. Pal B, Chen Y, Vaillant F, Capaldo BD, Joyce R, Song X, et al. A single-cell RNA expression atlas of normal, preneoplastic and tumorigenic states in the human breast. EMBO J. 2021;40:e107333.
20. Wu SZ, Al-Eryani G, Roden DL, Junankar S, Harvey K, Andersson A, et al. A single-cell and spatially resolved atlas of human breast cancers. Nat Genet. 2021;53:1334-47.
21. Borcherding N, Vishwakarma A, Voigt AP, Bellizzi A, Kaplan J, Nepple K, et al. Mapping the immune environment in clear cell renal carcinoma by single-cell genomics. Commun Biol. 2021;4:122.

22. Hoadley KA, Yau C, Hinoue T, Wolf DM, Lazar AJ, Drill E, et al. Cell-of-Origin Patterns Dominate the Molecular Classification of 10,000 Tumors from 33 Types of Cancer. Cell. 2018;173:291-304 e6.
23. Lanczky A, Gyorffy B. Web-Based Survival Analysis Tool Tailored for Medical Research (KMplot): Development and Implementation. J Med Internet Res. 2021;23:e27633.
24. Yoon CI, Ahn SG, Bae SJ, Shin YJ, Cha C, Park SE, et al. High A20 expression negatively impacts survival in patients with breast cancer. PLoS One. 2019;14:e0221721.
25. Wolff AC, Hammond MEH, Allison KH, Harvey BE, Mangu PB, Bartlett JM, et al. Human epidermal growth factor receptor 2 testing in breast cancer: American Society of Clinical Oncology/College of American Pathologists clinical practice guideline focused update. Archives of pathology & laboratory medicine. 2018;142:1364-82.
26. Nguyen QH, Pervolarakis N, Blake K, Ma D, Davis RT, James N, et al. Profiling human breast epithelial cells using single cell RNA sequencing identifies cell diversity. Nat Commun. 2018;9:2028.
27. Prat A, Perou CM. Mammary development meets cancer genomics. Nat Med. 2009;15:842-4.
28. Keller PJ, Arendt LM, Skibinski A, Logvinenko T, Klebba I, Dong S, et al. Defining the cellular precursors to human breast cancer. Proc Natl Acad Sci U S A. 2012;109:2772-7.
29. Proia TA, Keller PJ, Gupta PB, Klebba I, Jones AD, Sedic M, et al. Genetic predisposition directs breast cancer phenotype by dictating progenitor cell fate. Cell Stem Cell. 2011;8:149-63.
30. Molyneux G, Geyer FC, Magnay FA, McCarthy A, Kendrick H, Natrajan R, et al. BRCA1 basal-like breast cancers originate from luminal epithelial progenitors and not from basal stem cells. Cell Stem Cell. 2010;7:403-17.
31. Adriance MC, Inman JL, Petersen OW, Bissell MJ. Myoepithelial cells: good fences make good neighbors. Breast Cancer Res. 2005;7:190-7.
32. Sirka OK, Shamir ER, Ewald AJ. Myoepithelial cells are a dynamic barrier to epithelial dissemination. J Cell Biol. 2018;217:3368-81.
33. Uxa S, Castillo-Binder P, Kohler R, Stangner K, Muller GA, Engeland K. Ki-67 gene expression. Cell Death Differ. 2021;28:3357-70.

34. Depowski PL, Rosenthal SI, Brien TP, Stylos S, Johnson RL, Ross JS. Topoisomerase IIalpha expression in breast cancer: correlation with outcome variables. Mod Pathol. 2000;13:542-7.
35. Liberzon A, Birger C, Thorvaldsdottir H, Ghandi M, Mesirov JP, Tamayo P. The Molecular Signatures Database (MSigDB) hallmark gene set collection. Cell Syst. 2015;1:417-25.
36. Subramanian A, Tamayo P, Mootha VK, Mukherjee S, Ebert BL, Gillette MA, et al. Gene set enrichment analysis: a knowledge-based approach for interpreting genome-wide expression profiles. Proc Natl Acad Sci U S A. 2005;102:15545-50.
37. Richer JK, Lange CA, Manning NG, Owen G, Powell R, Horwitz KB. Convergence of progesterone with growth factor and cytokine signaling in breast cancer. Progesterone receptors regulate signal transducers and activators of transcription expression and activity. J Biol Chem. 1998;273:31317-26.
38. Kanehisa M, Goto S. KEGG: kyoto encyclopedia of genes and genomes. Nucleic Acids Res. 2000;28:27-30.
39. Gao R, Bai S, Henderson YC, Lin Y, Schalck A, Yan Y, et al. Delineating copy number and clonal substructure in human tumors from single-cell transcriptomes. Nature biotechnology. 2021;39:599-608.
40. Yu S, Kim T, Yoo KH, Kang K. The T47D cell line is an ideal experimental model to elucidate the progesterone-specific effects of a luminal A subtype of breast cancer. Biochem Biophys Res Commun. 2017;486:752-8.
41. Holliday DL, Speirs V. Choosing the right cell line for breast cancer research. Breast Cancer Res. 2011;13:215.
42. Liu SQ, Edgerton SM, Moore DH, Thor AD. Measures of cell turnover (proliferation and apoptosis) and their association with survival in breast cancer. Clinical Cancer Research. 2001;7:1716-23.
43. Qin J, Zhou Z, Chen W, Wang C, Zhang H, Ge G, et al. BAP1 promotes breast cancer cell proliferation and metastasis by deubiquitinating KLF5. Nat Commun. 2015;6:8471.
44. Ebright RY, Zachariah MA, Micalizzi DS, Wittner BS, Niederhoffer KL, Nieman LT, et al. HIF1A signaling selectively supports proliferation of breast cancer in the brain. Nat Commun. 2020;11:6311.

45. Zhang L, Qu J, Qi Y, Duan Y, Huang YW, Zhou Z, et al. EZH2 engages TGFbeta signaling to promote breast cancer bone metastasis via integrin beta1-FAK activation. Nat Commun. 2022;13:2543.
46. Jordan VC. Tamoxifen: a most unlikely pioneering medicine. Nature reviews Drug discovery. 2003;2:205-13.
47. Reimand J, Isserlin R, Voisin V, Kucera M, Tannus-Lopes C, Rostamianfar A, et al. Pathway enrichment analysis and visualization of omics data using g:Profiler, GSEA, Cytoscape and EnrichmentMap. Nat Protoc. 2019;14:482-517.
48. Ashburner M, Ball CA, Blake JA, Botstein D, Butler H, Cherry JM, et al. Gene ontology: tool for the unification of biology. The Gene Ontology Consortium. Nat Genet. 2000;25:25-9.
49. Kucera M, Isserlin R, Arkhangorodsky A, Bader GD. AutoAnnotate: A Cytoscape app for summarizing networks with semantic annotations. F1000Res. 2016;5:1717.
50. Shannon P, Markiel A, Ozier O, Baliga NS, Wang JT, Ramage D, et al. Cytoscape: a software environment for integrated models of biomolecular interaction networks. Genome Res. 2003;13:2498-504.
51. Li Z, Wei H, Li S, Wu P, Mao X. The Role of Progesterone Receptors in Breast Cancer. Drug Des Devel Ther. 2022;16:305-14.
52. Mohammed H, Russell IA, Stark R, Rueda OM, Hickey TE, Tarulli GA, et al. Progesterone receptor modulates ERα action in breast cancer. Nature. 2015;523:313-7.
53. Finlay-Schultz J, Gillen AE, Brechbuhl HM, Ivie JJ, Matthews SB, Jacobsen BM, et al. Breast Cancer Suppression by Progesterone Receptors Is Mediated by Their Modulation of Estrogen Receptors and RNA Polymerase III. Cancer Res. 2017;77:4934-46.
54. Creighton CJ, Kent Osborne C, van de Vijver MJ, Foekens JA, Klijn JG, Horlings HM, et al. Molecular profiles of progesterone receptor loss in human breast tumors. Breast Cancer Res Treat. 2009;114:287-99.
55. Langbein S, Frederiks WM, zur Hausen A, Popa J, Lehmann J, Weiss C, et al. Metastasis is promoted by a bioenergetic switch: new targets for progressive renal cell cancer. Int J Cancer. 2008;122:2422-8.

56. Stamova BS, Apperson M, Walker WL, Tian Y, Xu H, Adamczy P, et al. Identification and validation of suitable endogenous reference genes for gene expression studies in human peripheral blood. BMC Med Genomics. 2009;2:49.
57. Wang J, Yuan W, Chen Z, Wu S, Chen J, Ge J, et al. Overexpression of G6PD is associated with poor clinical outcome in gastric cancer. Tumour Biol. 2012;33:95-101.
58. Mele L, Paino F, Papaccio F, Regad T, Boocock D, Stiuso P, et al. A new inhibitor of glucose-6-phosphate dehydrogenase blocks pentose phosphate pathway and suppresses malignant proliferation and metastasis in vivo. Cell Death Dis. 2018;9:572.
59. Bose S, Huang Q, Ma Y, Wang L, Rivera GO, Ouyang Y, et al. G6PD inhibition sensitizes ovarian cancer cells to oxidative stress in the metastatic omental microenvironment. Cell Rep. 2022;39:111012.

# APPENDICES

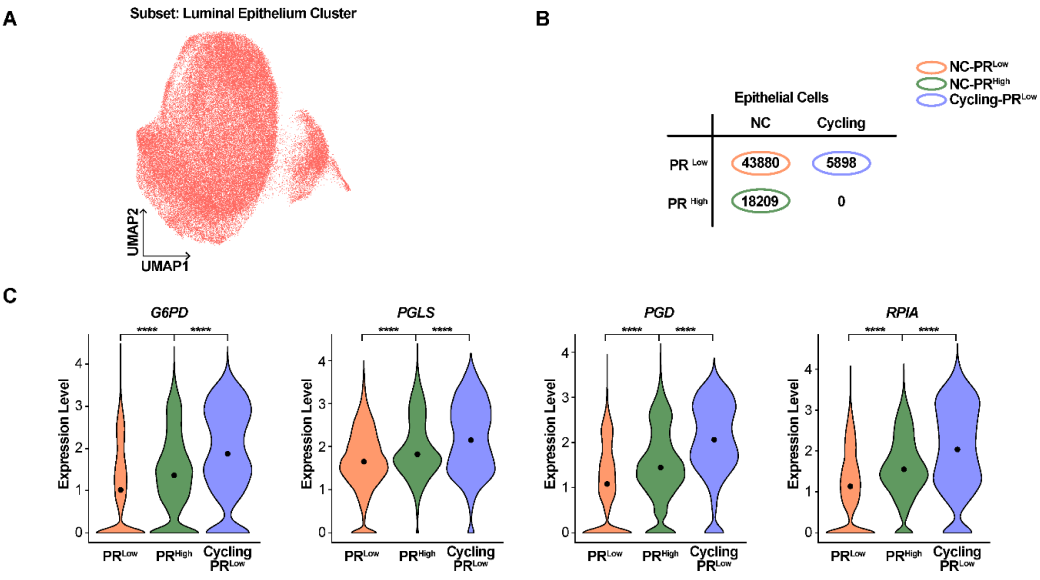


**Supplementary Fig. 1 Expression of PPP genes of luminal epithelial cells.**

**A** Dimension plot of luminal epithelial cells displaying subset from eight clusters. **B** Contingency table of luminal epithelial cells presenting cell count of NC and Cycling groups and PR Low, PR High groups. C Violin plots showing expression level of G6PD, PGLS, PGD and RPIA. The violin plots of **C** were presented as median expression value with adjusted *p* value. **** $p < 0.0001$.

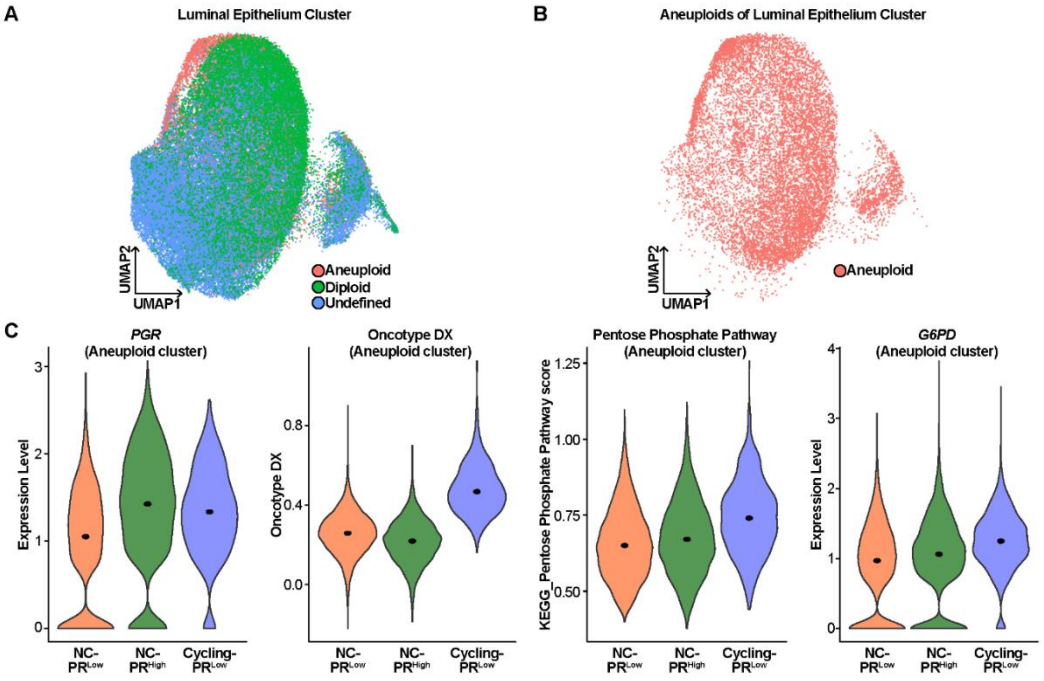


**Supplementary Fig. 2 Aneuploid cells of luminal epithelial cluster.**

**A** Dimension plot of luminal epithelial cluster showing Aneuploid, Diploid and Undefined cells divided by the result of CNV analysis. **B** Dimension plot of Aneuploid cells in the luminal epithelial cluster. **C** Violin plots presenting expression levels of PGR and G6PD, and score of Oncotype DX and Pentose Phosphate Pathway in Aneuploid cells.

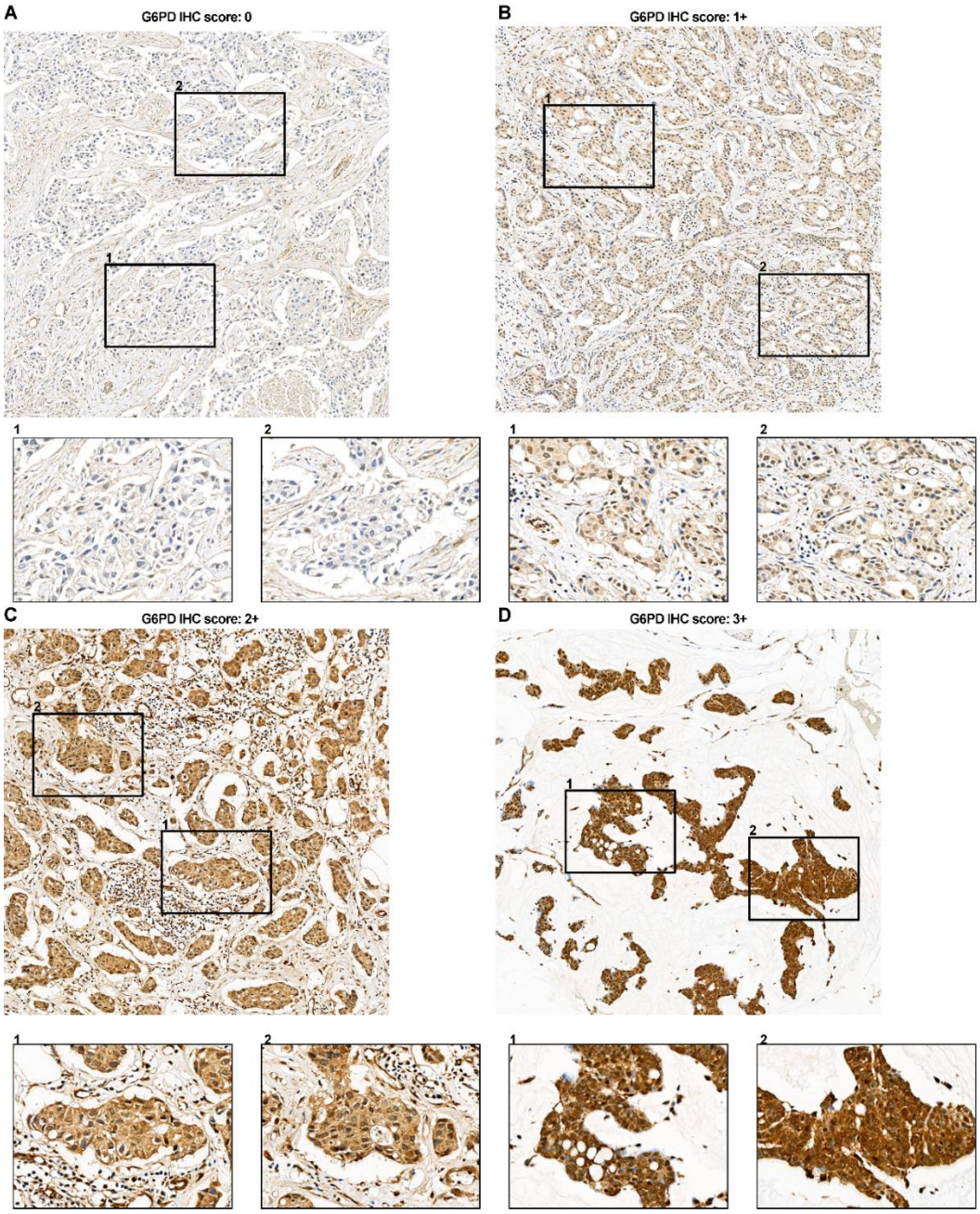


**Supplementary Fig. 3 IHC presenting G6PD expression in LA patients**

A The IHC presentation of G6PD expression was scored as 0, 1+, 2+, and 3+ (400x magnification).

The LA patients with a score of 0, 1+, were classified as belonging to the G6PD Low group. Conversely, the patients with a score of 2+ or 3+ were classified as belonging to the G6PD High group.

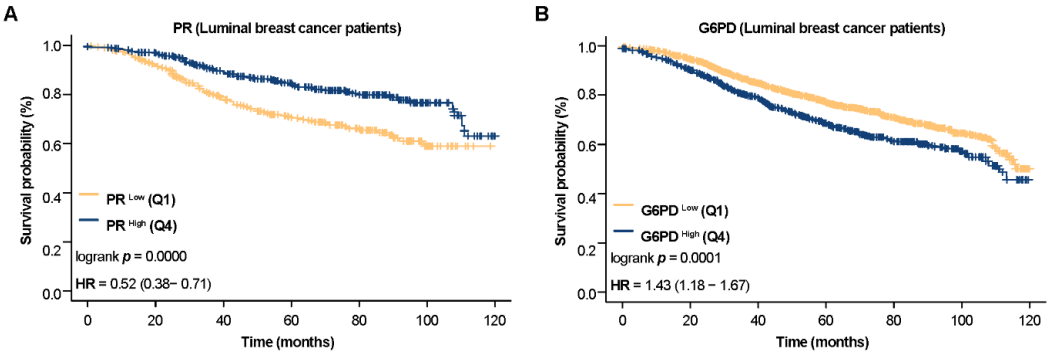


**Supplementary Fig. 4 Survival probabilities of luminal breast cancer patients based on PR and G6PD expression levels**

A-B Kaplan–Meier plots exhibiting the probability of luminal breast cancer patients of between PR $^{low}$ and PR $^{high}$ or between G6PD $^{low}$ and G6PD $^{high}$ from Kaplan-Meier plotter.

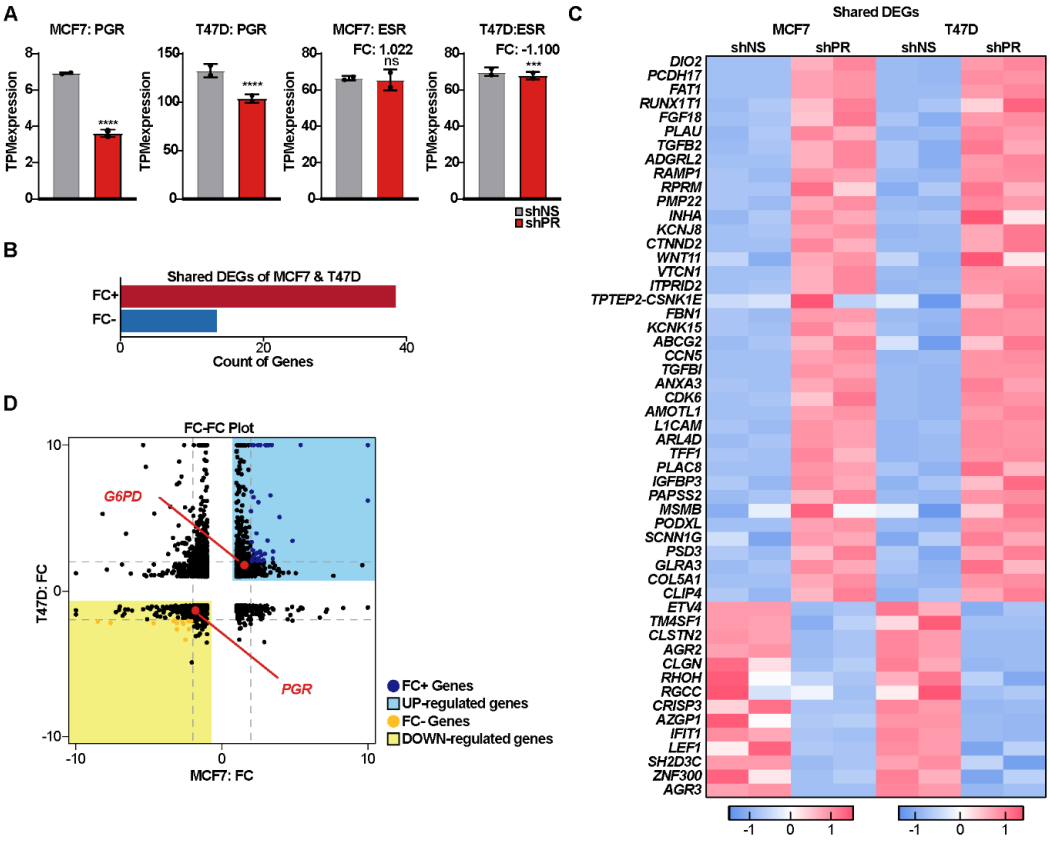


**Supplementary Fig. 5 Bulk RNA-seq presenting shared DEGs in PR KD cell lines.**

**A** Bar plots of PGR and ESR expression levels comparing between two groups. **B** Bar plot presenting shared DEGs (up-regulation: 39 genes, down-regulation: 14) in PR KD MCF7 and T47D. **C** Heatmap showing shared DEGs list of PR KD MCF7 and T47D. **D** Volcano plot displaying shared DEGs of PR KD MCF7 and T47D, marked with *PGR* and *G6PD*. *** $p < 0.001$, **** $p < 0.0001$.

A

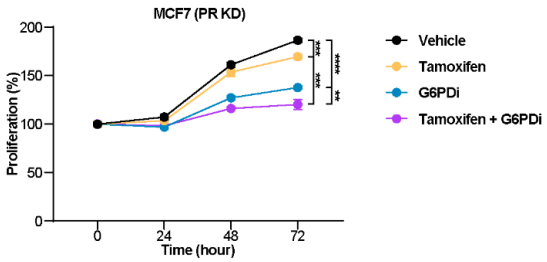


**Supplementary Fig. 6 Combination therapy of tamoxifen and G6PDi inhibiting aggressiveness of luminal breast cancer cells**

**A** Proliferation rate plot comparing vehicle, tamoxifen, G6PDi, and the combination of tamoxifen and G6PDi treatments in PR KD MCF7 cell. The proliferation rate was calculated as a relative value normalized to the 0-hour time point. The plot displays the mean values with standard deviations. ** $p < 0.01$, *** $p < 0.001$, **** $p < 0.0001$

Abstract in Korean

# 프로게스테론 수용체 억제에 의한 포도당-6-인산 탈수소효소 발현의 자극 및 루미날 유방암 악성도의 증가

유방암 중에서 루미날 유방암 (luminal breast cancer)은 가장 흔하고 예후가 좋은 아형입니다. 하지만, 프로게스테론 수용체 (progesterone receptor; PR)발현이 낮은 루미날 유방암 환자는 생존 확률이 낮고, 포도당의 높은 표준섭취값 (standard uptake value; SUV)과 관련이 있다는 보고가 있습니다. 그럼에도 불구하고, 프로게스테론 수용체와 루미날 유방암의 공격성 사이의 연관성에 대한 증거는 충분하지 않습니다.

루미날 유방암 (luminal breast cancer)은 유방암 가운데 가장 흔하고 예후가 좋은 아형입니다. 그러나 프로게스테론 수용체(progesterone receptor; PR)발현이 낮은 루미날 유방암 환자들은 생존율이 낮다는 보고가 있습니다. 그럼에도 불구하고, 프로게스테론 수용체와 루미날 유방암의 공격성 사이의 연관성에 대한 기전에 대한 충분한 증거는 아직 부족합니다. 우리는 프로게스테론 수용체와 [$^{18}$F] 플루오르데옥시글루코스 양전자 방출 단층촬영(FDG-PET)의 표준섭취계수(SUV) 간의 역상관 관계를 보여주는 이전 연구에 착안하여, PR 발현과 포도당 대사, 특히 오탄당 인산 경로(PPP) 사이의 잠재적 연관성을 확인하고자 했습니다. 이를 조사하기 위해, 우리는 공개된 데이터를 이용한 단일 세포 RNA 시퀀싱(scRNA-seq) 분석을 수행했습니다. 흥미롭게도, 분석 결과, 증식 활동이 증가하고 프로게스테론 스용체 발현이 감소한 특정 상피세포들이 오탄당 인산 경로와 포도당-6-인산 탈수소효소(glucose-6-phosphate dehydrogenase; G6PD) 발현의 활성을 증가시킨다는 사실을 발견했습니다. 이러한 결과를 검증하기 위해, 우리는 루미날 유방암 세포주인 MCF7 과 T47D 에서 프로게스테론 수용체 발현을 억제했으며, 그 결과 증식 속도와 포도당-6-인산 탈수소효소 발현을 동반한 오탄당 인산 경로의 활동이 가속화되었습니다. 우리는 프로게스테론 수용체의 발현이 억제 (knockdown; KD)된 세포에서 오탄당 인상 경로를 통한 포도당 이용을 촉진하여 유방암의 공격성을 증가시킬 것이라고 가설을 세웠습니다. 중요한 점은, 포도당-6-인산 탈수소효소의 특이 억제제로 치료한 결과, 프로게스테론 수용체 발현이 억제된 암세포의 공격성이 감소했다는 것입니다. 이러한 발견은 프로게스테론 수용체 발현이 낮은 공격적인 루미날 유방암에 대해 포도당-6-인산 탈수소효소를 표적으로 하는 치료 전략이 유망할 수 있음을 시사합니다.

---

**핵심되는 말** : 루미날 유방암, 프로게스테론 수용체, 포도당-6-인산 탈수소효소